IEEE Photonics Journal
An IEEE Photonics Society Publication

Open Access

Phase Retrieval for Digital Holographic Microscopy With Defocused Holograms

Volume 10, Number 1, February 2018

Dingnan Deng
Weijuan Qu
Wenqi He
Yu Wu
Xiaoli Liu
Xiang Peng

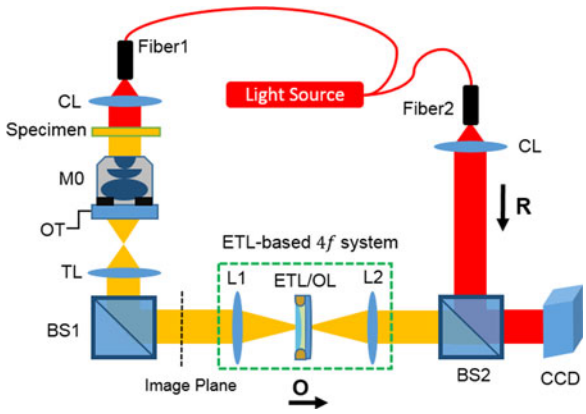

DOI: 10.1109/JPHOT.2017.2782674
1943-0655 © 2017 IEEE

IEEE photonics SOCIETY

IEEE

Phase Retrieval for Digital Holographic Microscopy With Defocused Holograms

Dingnan Deng,[1] **Weijuan Qu**,[2] **Wenqi He**,[1] **Yu Wu**,[1] **Xiaoli Liu**,[1] **and Xiang Peng**[1]

[1]College of Optoelectronics Engineering, Key Laboratory of Optoelectronic Devices and Systems of Ministry of Guangdong Province, Shenzhen University, Shenzhen 518060, China
[2]Ngee Ann Polytechnic, Singapore 5994892

DOI:10.1109/JPHOT.2017.2782674

Manuscript received October 31, 2017; revised December 4, 2017; accepted December 8, 2017. Date of publication December 12, 2017; date of current version January 5, 2018. This work was supported in part by the Sino-German cooperation group:Computational Imaging and Metrology:GZ 1391; in part by the National Natural Science Foundation of China under Grant 61171073, Grant 61307003 and Grant 61377017; in part by the Sino-German Center for the Research Promotion:GZ 760; and in part by the Natural Science Foundation of SZU under Grant 2016028 and by Science and Technology Innovation Commission of Shenzhen under Grant JCYJ20160520164642478. Corresponding author: Xiang Peng (E-mail: xpeng@szu.edu.cn).

Abstract: A new phase retrieval technique in digital holographic microscopy (DHM) with three defocused holograms is proposed. Given the defocusing distance, the phase distributions of tested specimen can be reconstructed with a simple algebraic equation. We have deduced this equation in detail. To avoid the manual operation, the defocused holograms can be flexibly and precisely obtained by introducing an electronically tunable lens based 4f system. This method is suitable for an on-axis hologram as well as the off-axis one but avoids the requirements for not only the iterative process, complex spectrum selection in off-axis DHM or additional phase-shifting devices in on-axis DHM but also the assumption of tested specimen or previous knowledge of the system. A series of simulations and the experimental results of the microlens array and water drop demonstrate the feasibility and effectiveness of the proposed method.

Index Terms: Holography, phase measurement, microscopy.

1. Introduction

DIGITAL holographic microscopy (DHM) has been shown great performance on noncontact label-free quantitative phase imaging (QPI), and has been widely applied in various fields, such as cells [1], [2], micro-lens array [3]. The phase retrieval methods for DHM can be categorized into Fourier transform (FT) and phase-shifting (PS) technique. Off-axis DHM can retrieve the phase distributions of tested specimen from single hologram with FT method [4], [5]. Thus, it is valuable for dynamic measurement in practice. However, the FT-based method always need to obtain the full $+1$ order with complex operation; otherwise, the frequency leakage would lead to measurement errors, especially for the off-axis DHM system with small tilt angle. The PS method, envisioned by Yamaguchi and Zhang [6], [7], can give an accurate phase measurement without the superimposition of different diffraction orders. Many works have been reported to enhance the performance of the PS method by reducing the needed phase shifts [8]–[11]. One common problem of these methods is that they

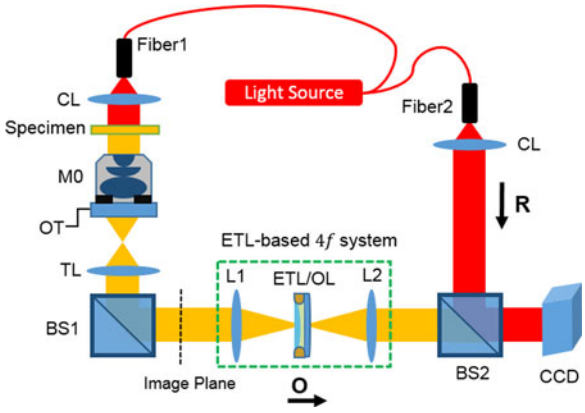

Fig. 1. Schematic of the experimental setup for the proposed method. CL, collimating lens; MO, microscope objective; OT, objective turret; TL, tube lens; L1, lens 1; L2, lens 2; ETL, electronically tunable lens; OL, offset lens; BS1, BS2, beam-splitter cubes; CCD, charge-coupled device.

have to introduce the phase shifts by different phase-shifting devices [12]–[15]. The phase shifting error [16] also may make the reconstructed object blurred.

Recently, many research works [17]–[20] have shown that the phase distributions can be retrieved with defocused images. From the point of view of defocus, defocused holograms obtained in different plane also can be used for reconstructing the phase distributions in DHM [21]–[29]. Phase-retrieval algorithms [21], [22] with two or more defocused holograms can reconstruct the whole optical wave field. However, the iterative process is time consuming. In contrast, the dual-plane methods [23]–[29] can achieve the purpose for QPI with two defocused holograms, which can avoid the requirements for iterative process, additional phase shifts, or complex spectrum selection. Two defocused holograms were recorded at two different planes separated by a small distance perpendicular to propagation direction, and later reconstructed using an algebraic manipulation in Fourier domain to remove the twin image noise. The zero order image can be eliminated by making an assumption of weak object wave [24], introducing a π shifting [25], [26], subtracting the average intensity of entire hologram [27], [28], or recording an additional known reference wave [29]. Nevertheless, these methods usually require many conditions such as the specific approximation of object, additional phase-shifting devices, or previous knowledge of system, these requirements would limit the application of defocused-holograms-based methods for phase retrieval in DHM.

In this paper, we propose an alternative phase retrieval technique in DHM with three defocused holograms. An ETL-based 4f system [30] was introduced to flexibly and precisely record the three defocused holograms that avoid the manual operation. Then the phase distributions of tested specimen can be reconstructed with a simple algebra equation. We have deduced this equation in details. The proposal with three defocused holograms avoids the requirements for not only the iterative process, complex spectrum selection in off-axis DHM or additional phase-shifting devices in on-axis DHM but also the assumption of weak object wave or previous knowledge of system. Some simulations demonstrate that the method can be applied for various DHM system, such as the off-axis, slightly off-axis, or on-axis. The proposal is also experimentally demonstrated via QPI of the micro-lens array and water drop.

2. Basic Principle

The experimental setup considered in our scheme is a transmission DHM system with the Mach-Zehnder interferometer configuration, as shown in Fig. 1. This study is verified on, but not limited to, this system. In the path of object wave (OW), a tested specimen is placed in the front focal plane of microscope objective (MO). After passing through the specimen, the OW was magnified by a

telescope system (comprised of a MO and a tube lens). The ETL-based 4f system, as shown in Fig. 1, consists of a standard 4f system with two lens (L1 and L2) and an ETL combined with an offset lens (OL) located at the Fourier plane, used to generate the defocused hologram. The OL was paired with the ETL and the composite lens ETL/OL can realize refocusing along positive and negative directions with respect to the intermediate image plane. The lens L1 relays the back focal plane of the MO onto the ETL/OL. The lens L2 reconstructs the final image at the CCD plane, which is conjugated with the image plane.

Three holograms with different defocusing distance z_1, z_2, z_3 recorded on CCD can be respectively written as

$$I_{z_1}(x_1, y_1) = \left|O_{z_1}\right|^2 + |R|^2 + O_{z_1}R^* + O_{z_1}^* R, \tag{1}$$

$$I_{z_2}(x_2, y_2) = \left|O_{z_2}\right|^2 + |R|^2 + O_{z_2}R^* + O_{z_2}^* R, \tag{2}$$

$$I_{z_3}(x_3, y_3) = \left|O_{z_3}\right|^2 + |R|^2 + O_{z_3}R^* + O_{z_3}{}^* R. \tag{3}$$

Here, O_{z_1}, O_{z_2} and O_{z_3} are the complex amplitude distribution of the OW $O(x, y)$ after propagation for different distance z_1, z_2, z_3. From the angular spectrum view point, the corresponding relation is given by

$$O_{z_i}(x_i, y_i) = F^{-1}\left\{F\left[O(x_i, y_i)\right] H_{z_i}\right\}, \tag{4}$$

where, $i = 1, 2, 3$ indicate O_{z_1}, O_{z_2} and O_{z_3}, respectively. $F\{\}$ and $F^{-1}\{\}$ denote the Fourier transform and inverse Fourier transform operators. H_{z_i} is the transfer function for free space propagation, which can be written as

$$H_{z_i}(\xi, \eta) = exp\left\{jkz_i\sqrt{1 - (\lambda\xi)^2 - (\lambda\eta)^2}\right\}. \tag{5}$$

Here, ξ and η are the spatial coordinates in the frequency domain. In our proposal, the relationship between the defocusing distance z_i and the focal length variations of ETL f_{ETL} can be established [30]:

$$z_i = \frac{f^2 \cdot (f_{ETL} + f_{OL} - d)}{f_{ETL} \cdot f_{OL}}, \tag{6}$$

where f is the focal length of two lens L1 and L2 ($f = f_{L1} = f_{L2}$), d is the axial distance between the ETL and OL, f_{OL} is the focal length of OL. Since f_{ETL} can be electronically controlled, the defocusing distance z_i can be easily adjusted whilst maintaining the position of the infocus image plane and image magnification.

According to the (5), the complex conjugate $(H_{z_i})^*$ of H_{z_i} equals to H_{-z_i}. From the (1)–(3), we can obtain:

$$I_{z_2} - I_{z_1} = A + (O_{z_2} - O_{z_1})R^* + (O_{z_2}^* - O_{z_1}^*)R, \tag{7}$$

$$I_{z_2} - I_{z_3} = B + (O_{z_2} - O_{z_3})R^* + (O_{z_2}^* - O_{z_3}^*)R, \tag{8}$$

where $A = |O_{z_2}|^2 - |O_{z_1}|^2$, $B = |O_{z_2}|^2 - |O_{z_3}|^2$. For simplicity, we can ignore the two terms A and B when the defocusing distance difference value $z_2 - z_1$ and $z_2 - z_3$ are very small. In addition, we assume that the given reference wave (RW) has the constant complex amplitude which will not change with the defocus of the holograms. It is because that the defocused holograms were generated by defocusing the object wave but not the reference wave. Thus, we can treat the OW and RW as a whole. In this case, after do the Fourier transform on the both side of (7) and (8), we can obtain:

$$F\left\{I_{z_2} - I_{z_1}\right\} = F\left\{O \cdot R^*\right\} \cdot (H_{z_2} - H_{z_1}) + F\left\{O^* \cdot R\right\} \cdot (H_{-z_2} - H_{-z_1}), \tag{9}$$

$$F\left\{I_{z_2} - I_{z_3}\right\} = F\left\{O \cdot R^*\right\} \cdot (H_{z_2} - H_{z_3}) + F\left\{O^* \cdot R\right\} \cdot (H_{-z_2} - H_{-z_3}). \tag{10}$$

Thus, the complex amplitude of $(O \cdot R^*)$ can be solved from (9) and (10):

$$O \cdot R^* = F^{-1}\left\{\frac{F\left\{I_{z_2} - I_{z_1}\right\} \cdot (H_{-z_2} - H_{-z_3}) - F\left\{I_{z_2} - I_{z_3}\right\} \cdot (H_{-z_2} - H_{-z_1})}{(H_{z_2} - H_{z_1}) \cdot (H_{-z_2} - H_{-z_3}) - (H_{z_2} - H_{z_3}) \cdot (H_{-z_2} - H_{-z_1})}\right\}. \tag{11}$$

Therefore, the retrieved phase can be expressed as

$$\varphi\ (O \cdot R^*) = \arctan\frac{\mathrm{Im}\left[O \cdot R^*\right]}{\mathrm{Re}\left[O \cdot R^*\right]}. \tag{12}$$

Here, "arctan" means the arc tangent operation, Im[·] and Re[·] are the imaginary part and the real part computation, respectively. The phase unwrapping method [31] is also applied to extend the wrapping phase into a continuous phase distribution. Based on the analysis of wavefront interference, the retrieved phase $\varphi(O \cdot R^*)$ can be written as [32]

$$\varphi\ (O \cdot R^*) = \varphi\left(O_{is}\right) + \varphi\left(R^*\right) + \varphi\left(O_t\right), \tag{13}$$

where $\varphi(O_{is})$ is the phase introduced by the imaging system in the object arm, $\varphi(R^*)$ is the phase of the conjugate RW, and $\varphi(O_t)$ is the phase introduced by the tested specimen. The term $\varphi(O_{is}) + \varphi(R^*)$ is system phase which coming from the differences between the OW and RW. Different system phases will produce different holograms. In our proposal, the imaging system in the object arm is a telescope system. After the imaging system, the OW without specimen can be assumed as a plane wave (PW). If the RW is PW, $\varphi(O_{is}) + \varphi(R^*)$ is the tilt phase aberration introduced by the off-axis angle of RW in off-axis DHM. For the spherical RW, $\varphi(O_{is}) + \varphi(R^*)$ is the parabolic phase aberration in on-axis DHM. To obtain the correct phase map of tested specimen, we also need to compensate the phase aberrations $\varphi(O_{is}) + \varphi(R^*)$ caused by the off-axis angle of planar RW or the spherical RW.

3. Simulations

A set of simulations have been carried out to verify the effectiveness of the proposed method. Fig. 2 shows the phase retrieval results obtained with the proposed method for the on-axis DHM. In this simulation, the wavelength of the light source is 658 nm and the simulated on-axis holograms with 256×256 square pixels. The amplitude and phase distributions of the simulated OW are shown in Fig. 2(a). Three holograms I_{z_1}, I_{z_2}, I_{z_3} are shown in Fig. 2(b), with different defocused distance $z_1 = -1$ μm, $z_2 = 0$ μm, $z_3 = 1$ μm, respectively. For the given defocusing distance, the root mean square error (RMSE) of A and B is 1.7242e-004 and 1.7242e-004, respectively. Thus, the defocusing distance difference $z_2 - z_1$ and $z_2 - z_3$ would be small enough to ignore the value A and B in (7) and (8). Fig. 2(c) shows the retrieved amplitude and phase distributions by the proposed method. The phase profiles along the white dotted line in Fig. 2(a) and (c) are shown in Fig. 2(d). Fig. 2(d) implies that our method can reconstruct the correct amplitude and phase distributions. Our proposal can eliminate the influence of zero order image and twin image noise in on-axis DHM. In addition, this method does not need to introduce the phase-shifting devices compared with the PS method [6], [7].

We also test our method for the off-axis DHM. Fig. 3 shows the phase retrieval results obtained with the proposed method for the off-axis DHM with small tilt angle. In this simulation, the wavelength of the light source is 658 nm and the simulated off-axis holograms with 456×456 square pixels. The sample interval is 4.4 μm. Fig. 3(a) shows the simulated specimen: micro-lens. We can set different defocusing distances $z_1 = -1$ μm, $z_2 = 0$ μm, $z_3 = 1$ μm, then three holograms I_{z_1}, I_{z_2}, I_{z_3} are obtained, as shown in Fig. 3(b)–(d), respectively. These different diffraction orders of hologram will superimpose because of the small off-axis tilt angle. Thus, we cannot retrieve the correct phase distributions of tested specimen with single hologram. In this simulation, the RMSE of A and B is 5.37281e-004 and 5.3634e-004, respectively. Thus, the two defocusing distance difference values $z_2 - z_1$ and $z_2 - z_3$ are small enough to ignore the value A and B in (7) and (8). Fig. 3(c) shows the retrieved phase map with the proposed method. The phase profiles along the white dotted line in

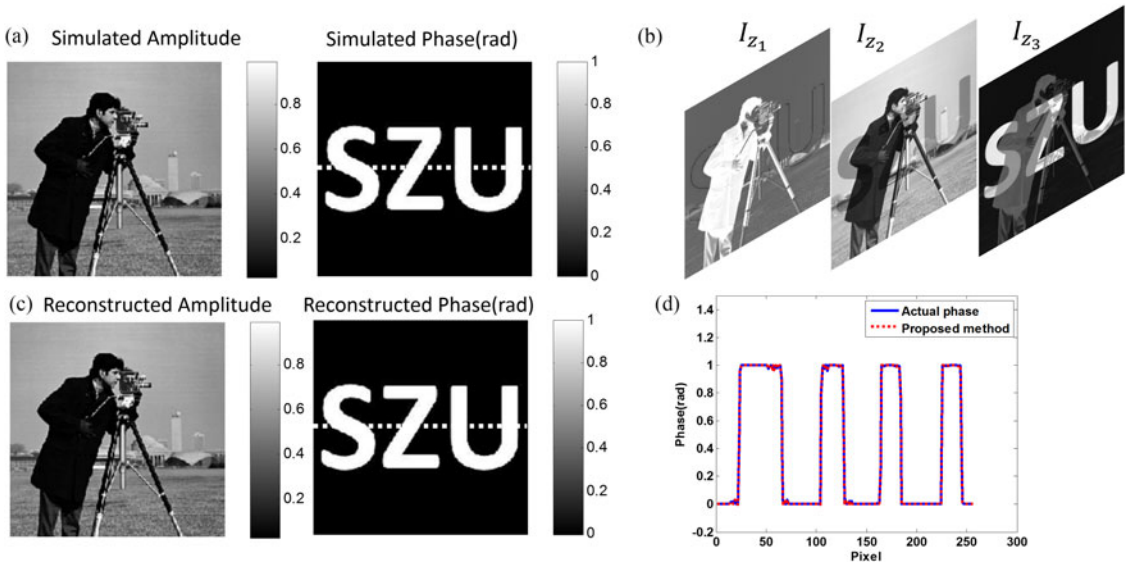

Fig. 2. Simulation analysis of the proposed method for the on-axis DHM. (a) Simulated amplitude and phase distributions; (b) Three holograms with different defocusing distances; (c) Reconstructed amplitude and phase distributions of the OW. The phase profiles along the white dotted line in (a) and (c) are plotted in panel (d).

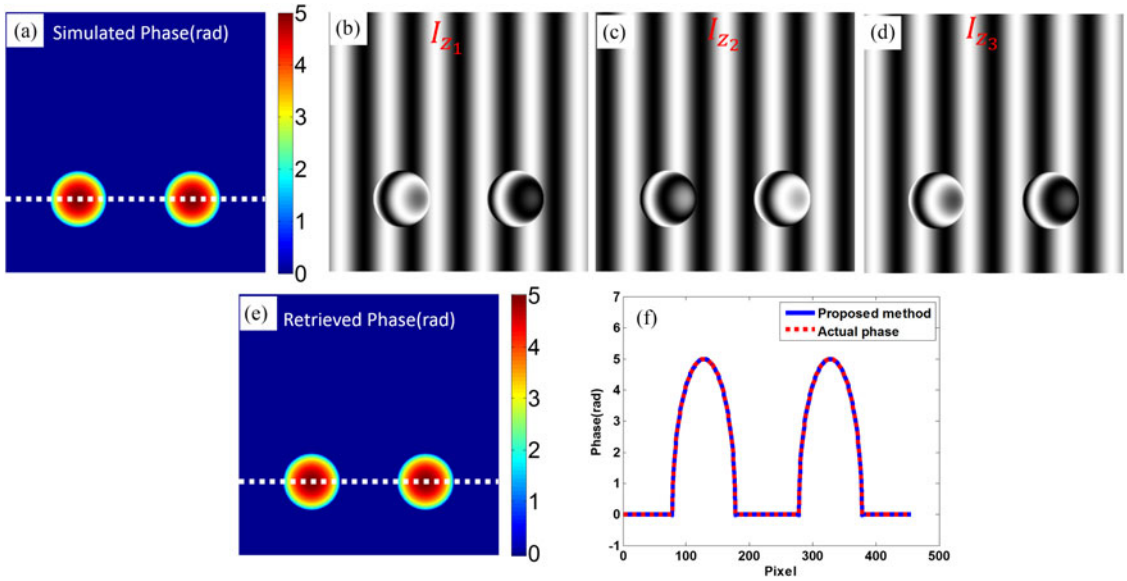

Fig. 3. Simulation analysis of the proposed method for the off-axis DHM with small tilt angle. (a) Simulated phase map; (b) The hologram with defocusing distance $z_1 = -1$ μm; (c) The infocus hologram ($z_2 = 0$ μm); (d) The hologram with defocusing distance $z_3 = 1$ μm; (e) Retrieved phase map; The phase profiles in (a) and (c) are plotted on panel (f).

Fig. 3(a) and (e) are shown in Fig. 3(f). Fig. 3(f) shows that our method also suitable for the off-axis DHM with small tilt angle but without the complex spectrum selection and obtain the accurate phase measurement.

In addition, we tested our method for off-axis DHM with different tilt angles. The different off-axis angles between the objet wave and reference wave will produce different holograms. Fig. 4(a)–(c)

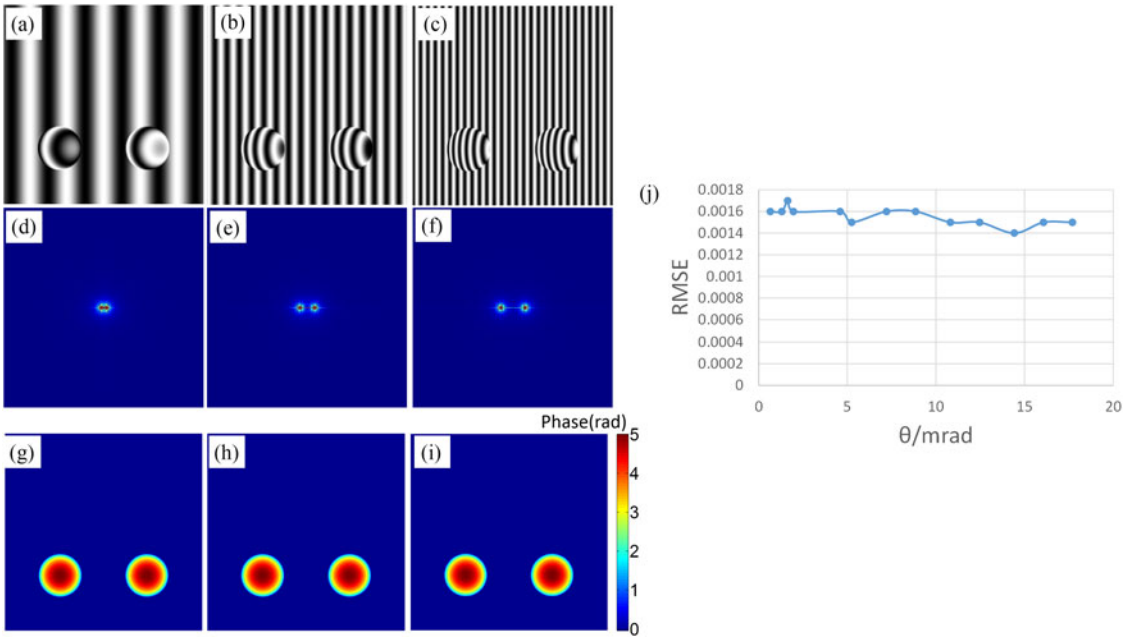

Fig. 4. Simulation analysis for off-axis DHM with different off-axis angles. The infocus hologram [(a), (b), (c)], Fourier spectrum of the hologram [(d), (e), (f)], and retrieved phase map [(g), (h), (i)] of the tested specimen, obtained when $\theta = 1.96,\ 5.25$ and 8.85 mrad. (j) The tilt angle variation versus the RMSE.

shows the infocus hologram when the tilt angle θ is equal to 1.96 mrad, 5.25 mrad, 8.85 mrad, respectively. The tilt angle also can be acquired from the spectrum of hologram [29]. The corresponding Fourier spectrum images are shown in Fig. 4(d)–(f), respectively. For different tilt angles, we respectively record three holograms with different defocusing distances $z_1 = -1$ μm, $z_2 = 0$ μm, $z_3 = 1$ μm. According the proposed method, the corresponding retrieved phase maps are shown in Fig. 4(g)–(i), respectively. The quality of the reconstructed phase maps is quantitatively measured with the RMSE, and the corresponding RMSE is 0.0016 rad, 0.0015 rad, and 0.0016 rad, respectively. In previous study [29], the dual plane method with the known reference wave will be affected by the off-axis angle and only efficient for off-axis DHM with small offset angle. The variations of RMSE with the tilt angle θ is shown in Fig. 4(j). As can be seen in Fig. 4(j), the retrieved phase obtained with the proposed method will not be affected by the different off-axis angles. The main reason is that the influence of reference wave has been previously eliminated by the subtraction operator from the defocused holograms (see (7), (8)) in our proposed method. In other word, the proposed method is suitable for off-axis DHM with larger off-axis angle.

4. Experiments

Experiments on the micro-lens array (SUSS, Micro-lens Array Nr.18-0092) were performed to demonstrate the effectiveness of our scheme. The wavelength of the light source is 658 nm and a CCD sensor with 1200 × 1600 square pixel of 4.4 μm in size used to record the hologram. The telescope system comprised of a 10× MO and a tube lens with focal length $f_{TL} = 100$ mm. The ETL-based 4f system, comprised a standard 4f system with two lens ($f_{L1} = f_{L2} = 150$ mm) and an ETL (Optotune AG, EL-10-30-C-VIS-LD) combined with an OL ($f_{OL} = -150$ mm) located at the Fourier plane of lens L1, can be flexible to generate holograms with different defocusing distances. The axial distance d is about 4 mm and it is so small that we consider the composite lens ETL/OL as "thin" for simplicity. Our experiment system is calibrated by a 1 mm/100 divisions stage micrometer. The calibration results show that the actual magnification of system is 6×.

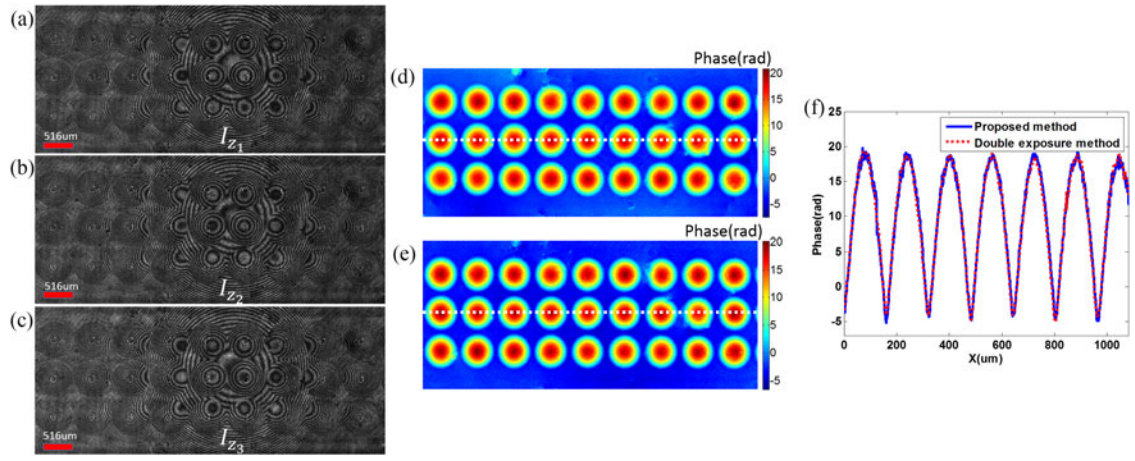

Fig. 5. Experiment results of micro-lens array obtained with the proposed method for on-axis DHM. (a) The defocused hologram $I_{z_1}(z_1 = -0.2\ \mu m)$; (b) The infocus hologram $I_{z_2}(z_2 = 0\ \mu m)$; (c) The defocused hologram $I_{z_3}(z_3 = 0.2\ \mu m)$. Retrieved phase map by (d) proposed method, (e) double exposure method. Phase profiles along the white-dotted line in (d) and (e) are plotted in panel (f).

We can generate different defocused holograms by changing the driven current of ETL. Based on the calibration of ETL, we found that the focal length of ETL versus its driven current changes appears to be a nonlinear relationship. The relationship between the focal length f_{ETL} (mm) and the driven current T(mA) can be written as [33]

$$f_{ETL}(T) = 0.001478 \cdot T^2 - 0.8505 \cdot T + 208.6. \tag{14}$$

In addition, the ETL also has good reproducibility and it does not introduce its own phase error [34]. Thus, we can precisely record defocused holograms with different defocusing distances.

Fig. 5 shows the on-axis holograms recorded by the proposed experiment system for tested specimen. In this experiment, the RW is a spherical wave that produces the on-axis circular hologram. The defocused hologram $I_{z_1}(z_1 = -0.2\ \mu m)$ is shown in Fig. 5(a). Fig. 5(b) shows the infocus hologram $I_{z_2}(z_2 = 0\ \mu m)$. Fig. 5(c) shows the on-axis hologram I_{z_3} with defocusing distance $z_3 = 0.2\ \mu m$. Based on the (6) and (14), the corresponding driven current of ETL T_{z_1}, T_{z_2} and T_{z_3} is 73.30 mA, 73.62 mA, 73.94 mA, respectively. It is clearly seen that we cannot retrieve the correct phase distributions of tested specimen from single on-axis hologram due to the superimposition of different diffraction orders. Otherwise, one needs to obtain the phase-shifting holograms with additional phase-shifting devices. As mentioned above, the spherical RW will also introduce the parabolic phase aberration on the retrieved phase, which can be numerically compensated [35]. Then we can obtain the correct phase map. For the given defocusing distance z_1, z_2 and z_3, the RMSE of A and B is 0.0546 and 0.0546, respectively. Thus, the two defocusing distance difference values $z_2 - z_1$ and $z_2 - z_3$ are small enough to ignore the value A and B in (7) and (8). The retrieved phase map of micro-lens array retrieved with the proposed method is shown in Fig. 5(d). Before the experiment, we measure the micro-lens array with double exposure method [36] in advance. The retrieved phase map is shown in Fig. 5(e). The phase profiles along the white-dotted line in Fig. 5(d) and (e) are shown in Fig. 5(f). It is clearly shown that the phase distributions measured by both methods are comparable. These experimental results also demonstrate that our proposal with three defocused holograms can obtain the accurate phase measurement without requirements for additional phase-shifting devices in on-axis DHM.

Finally, we test the proposed method for off-axis DHM with water drop. Fig. 6 shows the experiment results of the water drop. In this experiment, the RW is PW which avoid the influence of the parabolic phase aberration but introduce the tilt phase aberration due to the off-axis angle of RW. Fig. 6(a) shows the off-axis hologram I_{z_1} with defocusing distance $z_1 = 0.1\ \mu m$. The defocusing hologram

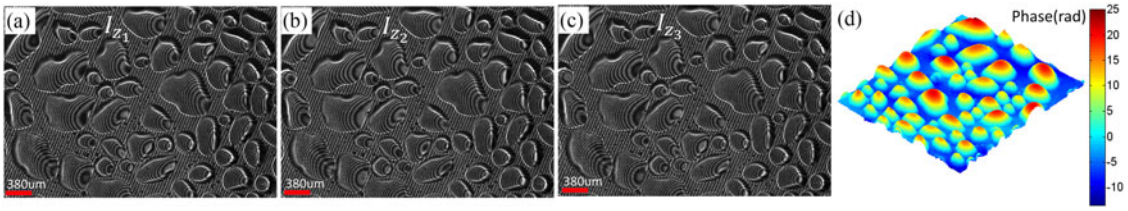

Fig. 6. Experiment results of water drop obtained with the proposed method for off-axis DHM. (a) The defocused hologram $I_{z_1}(z_1 = 0.1\ \mu m)$; (b) The defocused hologram $I_{z_2}(z_2 = 0.2\ \mu m)$; (c) The defocused hologram $I_{z_3}(z_3 = 0.3\ \mu m)$; (d) Retrieved phase map.

$I_{z_2}(z_2 = 0.2\ \mu m)$ is shown in Fig. 6(b). Fig. 6(c) shows the off-axis hologram I_{z_3} with defocusing distance $z_3 = 0.3\ \mu m$. According to the (6) and (16), the corresponding driven current of ETL T_{z_1}, T_{z_2} and T_{z_3} is 73.78 mA, 73.94 mA, 74.10 mA, respectively. As mentioned above, we can numerically compensate the off-axis tilt to obtain the correct phase map [35]. Fig. 6(d) shows the retrieved phase map obtained with the proposed method. These results show that the proposed method can retrieve the phase distributions of tested specimen with three defocused holograms. This method can avoid the requirements for complex spectrum selection in off-axis DHM.

5. Conclusion

In conclusion, we reported a new phase retrieval method based on three defocused holograms for QPI in DHM. We have deduced a simple algebra equation from three defocused holograms to retrieve the phase distributions of tested specimen, which can eliminate the influence of zero order image and twin image noise. The proposal can avoid the requirement for not only the iterative process, complex spectrum selection in off-axis DHM or additional phase-shifting devices in on-axis DHM but also the assumption of object or previous knowledge of system. The defocused holograms can be obtained by an ETL-based 4f system without manual operation. Simple and effective performance makes the approach available for different DHM systems, such as the off-axis, slightly off-axis, or on-axis. The simulation results for on-axis and off-axis DHM agree well with the theoretical analysis. The experimental results of the micro-lens and the water drop for QPI demonstrate the validity and effectiveness of our proposed method.

Acknowledgment

The first author thanks the internship program of Ngee Ann Polytechnic.

References

[1] B. Rappaz, P. Marquet, E. Cuche, Y. Emery, C. Depeursinge, and P. J. Magistretti, "Measurement of the integral refractive index and dynamic cell morphometry of living cells with digital holographic microscopy," *Opt. Express*, vol. 13, no. 23, pp. 9361–9373, Nov. 2005.
[2] A. Anand, V. K. Chhaniwal, and B. Javidi, "Imaging embryonic stem cell dynamicsusing quantitative 3-D digital holographic microscopy," *IEEE Photon. J.*, vol. 3, no. 3, pp. 546–554, Jun. 2011.
[3] W. J. Qu, O. C. Chee, Y. J. Yu, and A. Asundi, "Characterization and inspection of microlens array by single cube beam splitter microscopy," *Appl. Opt.*, vol. 50, no. 6, pp. 886–890, Feb. 2011.
[4] M. Takeda, H. Ina, and S. Kobayashi, "Fourier-transform method of fringe-patternanalysis for computer-based topography and interferometry," *J. Opt. Soc. Amer.*, vol. 72, no. 1, pp. 156–160, Jan. 1982.
[5] E. Cuche, P. Marquet, and C. Depeursinge, "Simultaneous amplitude-contrast and quantitative phase-contrast microscopy by numerical reconstruction of Fresnel off-axis holograms," *Appl. Opt.*, vol. 38, no. 34, pp. 6994–7001, Dec. 1999.
[6] I. Yamaguchi and T. Zhang, "Phase-shifting digital holography," *Opt. Lett.*, vol. 22, no. 16, pp. 1268–1270, Aug. 1997.
[7] I. Yamaguchi, T. Ida, M. Yokota, and K. Yamashita, "Surface shape measurement by phase-shifting digital holography with a wavelength shift," *Appl. Opt.*, vol. 45, no. 29, pp. 7610–7616, Oct. 2006.

[8] X. F. Meng *et al.*, "Two-step phase-shifting interferometry and its application in image encryption," *Opt. Lett.*, vol. 31, no. 10, pp. 1414–1416, May 2006.
[9] J. P. Liu and T. C. Poon, "Two-step-only quadrature phase-shifting digital holography," *Opt. Lett.*, vol. 34, no. 3, pp. 250–252, Feb. 2009.
[10] G. L. Chen, C. Y. Lin, H. F. Yau, M. K. Kuo, and C. C. Chang, "Wave-front reconstruction without twin-image blurring by two arbitrary step digital holograms," *Opt. Express*, vol. 15, no. 18, pp. 11601–11607, Sep. 2007.
[11] N. T. Shaked, Y. Zhu, M. T. Rinehart, and A. Wax, "Two-step-only phase-shifting interferometry with optimized detector bandwidth for microscopy of live cells," *Opt. Express*, vol. 17, no. 18, pp. 15585–15591, Aug. 2009.
[12] T. D. Yang, H. J. Kim, K. J. Lee, B. M. Kim, and Y. Choi, "Single-shot and phase-shifting digital holographic microscopy using a 2-Dgrating," *Opt. Express*, vol. 24, no. 9, pp. 9480–9488, May 2016.
[13] D. Malacara, M. Servín, and Z. Malacara, *Interferogram Analysis For Optical Testing*. Boca Raton, FL, USA: CRC Press, 2005.
[14] T. Xi *et al.*, "Phase-shifting infrared digital holographic microscopy based on an all-fiber variable phase shifter," *Appl. Opt.*, vol. 56, no. 10, pp. 2686–2690, Apr. 2017.
[15] Y. Bitou, "Digital phase-shifting interferometer with an electrically addressed liquid-crystal spatial light modulator," *Opt. Lett.*, vol. 28, no. 7, pp. 1576–1578, Sep. 2003.
[16] C. S. Guo, L. Zhang, H. T. Wang, J. Liao, and Y. Y. Zhu, "Phase-shifting error and its elimination in phase-shifting digital holography," *Opt. Lett.*, vol. 27, no. 19, pp. 1687–1689, Oct. 2002.
[17] L. J. Allen and M. P. Oxley, "Phase retrieval from series of images obtained by defocus variation," *Opt. Commun.*, vol. 199, no. 1, pp. 65–75, Nov. 2001.
[18] M. Ryabko *et al.*, "Throughfocus scanning optical microscopy (TSOM) considering optical aberrations: practical implementation," *Opt. Express*, vol. 23, no. 25, pp. 32215–32221, Dec. 2015.
[19] M. Hirose, K. Shimomura, A. Suzuki, N. Burdet, and Y. Takahashi, "Multiple defocused coherent diffraction imaging: Method for simultaneously reconstructing objects and probe using X-ray free-electron lasers," *Opt. Express*, vol. 24, no. 11, pp. 11917–11925, May 2016.
[20] H. Wang *et al.*, "Computational out-of-focus imaging increases the space–bandwidth product in lens-based coherent microscopy," *Opt.*, vol. 3, no. 12, pp. 1422–1429, Dec. 2016.
[21] G. Liu and P. D. Scott, "Phase retrieval and twin-image elimination for in-line Fresnel holograms," *J. Opt. Soc. Amer. A.*, vol. 4, no. 1, pp. 159–165, Jan.1987.
[22] Y. Zhang, G. Pedrini, W. Osten, and H. Tiziani, "Whole optical wave field reconstruction from double or multi in-line holograms by phase retrieval algorithm," *Opt. Express*, vol. 11, no. 24, pp. 3234–3241, Dec. 2003.
[23] Y. Zhang and X. Zhang, "Reconstruction of a complex object from two in-line holograms," *Opt. Express*, vol. 11, no. 6, pp. 572–578, Mar. 2003.
[24] Y. Zhang, G. Pedrini, W. Osten, and H. Tiziani, "Reconstruction of in-line digital holograms from two intensity measurements," *Opt. Lett.*, vol. 29, no. 15, pp. 1787–1789, Aug. 2004.
[25] B. Das, C. S. Yelleswarapu, and D. V. G. L. Rao, "Quantitative phase microscopy using dual-plane in-line digital holography," *Appl. Opt.*, vol. 51, no. 9, pp. 1387–1396, Mar. 2012.
[26] B. Das and C. S. Yelleswarapu, "Dual plane in-line digital holographic microscopy," *Opt. Lett.*, vol. 35, no. 20, pp. 3426–3428, Oct. 2010.
[27] G. Situ, J. P. Ryle, U. Gopinathan, and J. T. Sheridan, "Generalized in-line digital holographic technique based on intensity measurements at two different planes," *Appl. Opt.*, vol. 47, no. 5, pp. 711–717, Feb. 2008.
[28] J. H. Han, R. P. Li, J. H. Liu, F. S. Hai, and M. J. Huang, "Two-step phase shifting differential-recording digital holographic microscopy," *Sci. Rep.*, vol. 7, no. 1, May 2017, Art. no. 1992.
[29] F. Wang, D. Wang, S. Panezai, L. Rong, Y. Wang, and J. Zhao, "Generalized dual-plane digital holographic imaging method," *Opt. Commun.*, vol. 381, pp. 56–62, Jul. 2016.
[30] C. Zuo, Q. Chen, W. Qu, and A. Asundi, "High-speed transport-ofintensity phase microscopy with an electrically tunable lens," *Opt. Express*, vol. 21, no., pp. 24060–24075, Oct. 2013.
[31] D. C. Ghiglia and M. D. Pritt, *Two-Dimensional Phase Unwrapping: Theory, Algorithms, and Software*. Hoboken, NJ, USA: Wiley, 1998.
[32] W. Qu *et al.*, "Physical spherical phase compensation in reflection digital holographic microscopy," *Opt. Laser Eng.*, vol. 50, no. 4, pp. 563–567, Jul. 2011.
[33] Z. Wang, W. Qu, F. Yang, and A. Asundi, "Focal length calibration of an electrically tunable lens by digital holography," *Appl. Opt.*, vol. 55, no. 4, pp. 749–756, Feb. 2016.
[34] D. Deng *et al.*, "Simple and flexible phase compensation for digital holographic microscopy with electrically tunable lens," *Appl. Opt.*, vol. 56, no. 21, pp. 6007–6014, Jul. 2017.
[35] T. Colomb *et al.*, "Numerical parametric lens for shifting, magnification, and complete compensation in digital microscopy," *J. Opt. Soc. Amer. A.*, vol. 23, no. 12, pp. 3177–3190, Dec. 2006.
[36] P. Ferraro *et al.*, "Compensation of the inherent wave front curvature in digital holographic coherent microscopy for quantitative phase-contrast imaging," *Appl. Opt.*, vol. 42, no. 11, pp. 1938–1946, Apr. 2003.